快速蛋白質結晶條件篩選系統

Rapid Protein Crystallization by a Micro Osmotic Screening System

以滲透壓控制水分子穿過半透膜的流動，動態調節蛋白質結晶過程中各項濃度的變化，使用少量樣本即可快速並反覆篩選適當的結晶條件；本研究所開發的雛型為6 × 8陣列，體積為 20 × 24 × 2.5 mm^3，已成功應用在四種蛋白質結晶條件的篩選，使用20 μL的樣本，在二至六小時內順利產生蛋白質結晶。

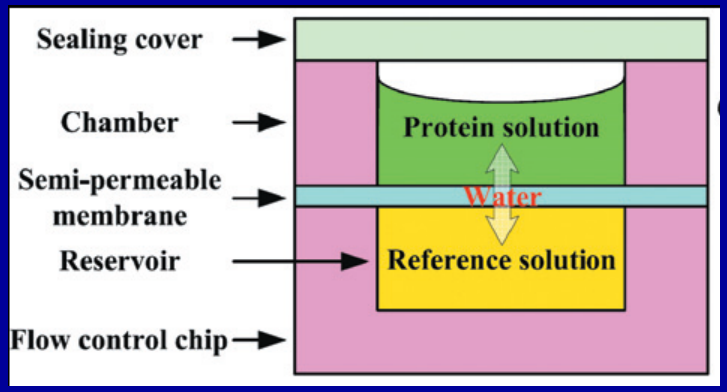

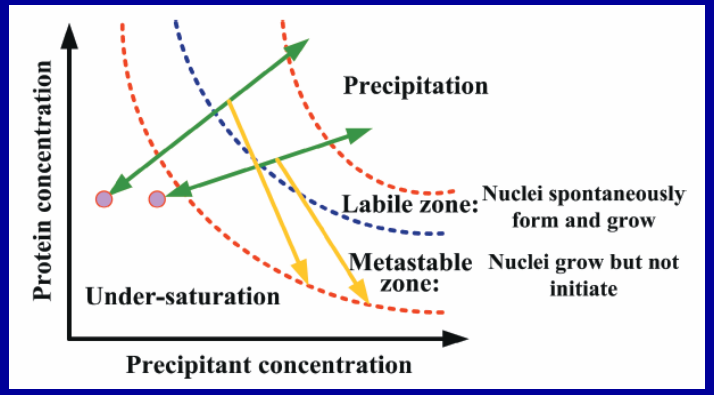

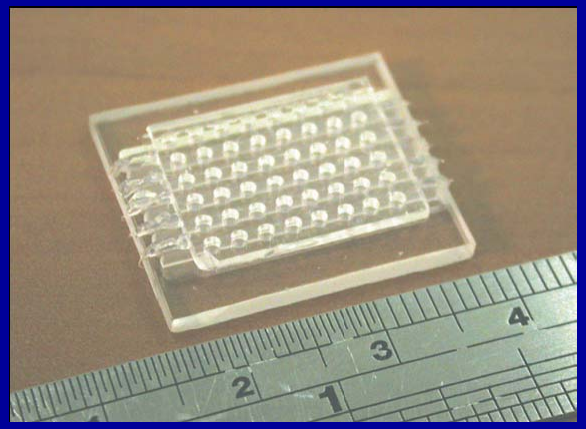

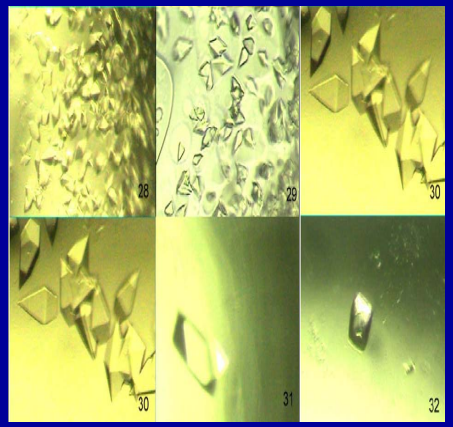

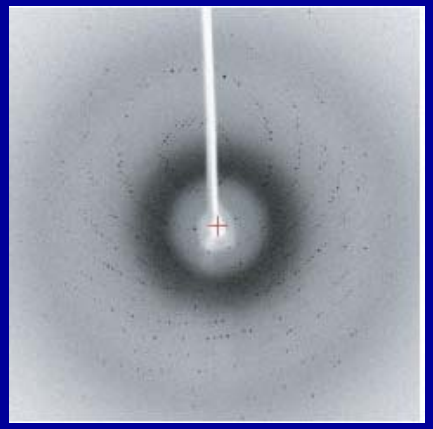

IOP Publishing Journal of Micromechanics and Microengineering
J. Micromech. Microeng. **17** (2007) 642–650 doi:10.1088/0960-1317/17/3/029

Rapid protein crystallization by a micro osmotic screening system*

Po-Hsiung Chan and Yu-Chuan Su

Department of Engineering and System Science, National Tsing Hua University, Hsinchu, Taiwan

E-mail: ycsu@ess.nthu.edu.tw

Received 20 October 2006, in final form 29 January 2007
Published 20 February 2007
Online at stacks.iop.org/JMM/17/642

Abstract
This work presents a micro osmotic screening system that grows protein crystals in hours while consuming only micrograms of samples. Throughout the crystallization process, water can be driven in or out of a protein solution (across a semi-permeable membrane) to adjust its concentrations as desired. With the bi-directional and adjustable flow control realized by osmosis, each protein sample can be screened for crystallization conditions over a highly extended range. In the prototype demonstration, 6×8 screening arrays having an overall size of $20 \times 24 \times 2.5$ mm^3 were fabricated and characterized with crystallization experiments. In these experiments, crystallization conditions for four proteins, including lysozyme, catalase, thaumatin and xylanase, were identified within 2–6 h while consuming less than 20 μl of sample solution for each protein. Furthermore, it was also demonstrated that diffraction-quality crystals may be grown and harvested from the prototype system. As such, this osmotic system pioneers a new class of rapid screening schemes for high-throughput protein crystallization.

(Some figures in this article are in colour only in the electronic version)

Introduction

In the post-genomic era, particularly challenging work is to investigate the structure–function relationship of encoded proteins on a genome-wide scale [1]. The structural information of proteins has proven to be valuable in unraveling clues to their functions, which are critical for the treatment of many diseases, but undetectable from primary sequence analysis. Once the structure–function relationship of a disease-related protein is unveiled, it may significantly facilitate the development of rationally designed drugs for the disease [2, 3]. Protein x-ray crystallography, which has proven to be a versatile detection method in structural genomics, is a technique in which the patterns produced by the diffraction of x-rays through protein crystals are analyzed to reveal their molecular structures [4]. In order to accelerate the detecting process, researches are being conducting by optimizing and automating each individual step, including protein expression and purification, robotics crystallization technologies, and data collection by synchrotron beam-lines, as well as improved methods for solving structures [5, 6]. Despite these efforts, the determination of protein structures remains a laborious and often unreliable task, mainly because of the difficulty in growing diffraction-quality crystals. Until now, the growth of protein crystals is still mostly empirical and remains the most labor-intensive and rate-limiting step, which requires automation, miniaturization and parallelization in order to reach the capacity necessary for high-speed and large-scale structure determination efforts.

Traditionally, protein crystals are grown by methods such as hanging-drop vapor diffusion, microbatch, dialysis and free interface diffusion [7–9]. These crystallization techniques typically use microliters of concentrated protein solution per assay, necessitating milligram quantities of sample materials for crystallization screening trials. Microfluidics, or lab-on-a-chip technology, is proving to be a powerful, rapid and efficient approach to a wide variety of bio-analytical applications [10, 11]. The low materials consumption, combined with the potential for packing a large number of experiments in a few cubic centimeters, makes it an attractive technique

* A portion of this paper was presented at the 10th International Conference on Miniaturized Systems for Chemistry and Life Sciences, Tokyo, Japan, November 2006.

for both initial screening and subsequent optimization of macromolecular crystallization conditions [12]. Previously, researchers have proposed various microfluidic schemes, such as free interface diffusion [13] and microbatch [14], for high-throughput protein crystallization. Although these approaches are capable of setting up hundreds of nanoliter-sized trials in minutes, the overall sample consumptions remain high if each trial can only screen for a limited range of crystallization conditions. Furthermore, the lack of controllability over the crystallization process has made it difficult to optimize the conditions for growing diffraction-quality protein crystals.

To address this need, this work presents a new osmotic screening scheme that is capable of controlling and optimizing the crystallization process to rapidly grow diffraction-quality protein crystals with minimum sample consumption. Three accomplishments have been achieved: (1) the employment of a bi-directional flow control mechanism, which is realized by osmosis, to adjust the concentrations of protein solutions and promote the growth of protein crystals as desired; (2) a comprehensive scheme that highly extends the screening ranges of crystallization conditions for each protein assay and (3) a rapid and effective protein crystallization system that grows protein crystals in hours with only microgram sample consumption. As such, this osmotic system pioneers a new class of rapid screening schemes for high-throughput protein crystallization.

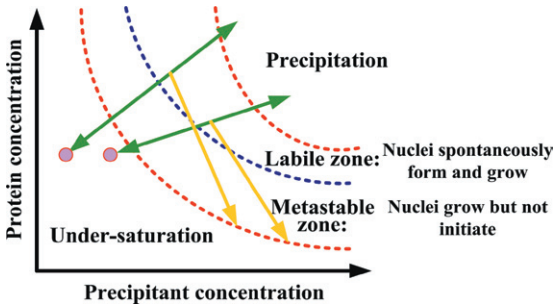

Figure 1. A simplified two-dimensional phase diagram with trajectories of two osmotic crystallization processes sketched on it.

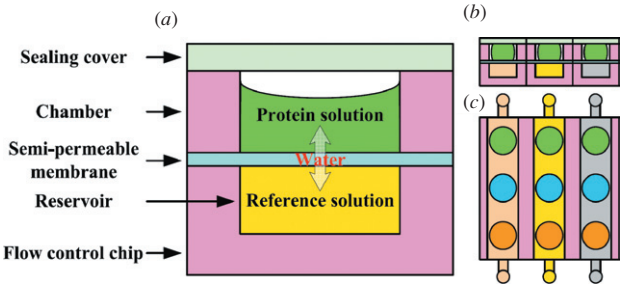

Figure 2. Structure of the osmotic screening system: (*a*) and (*b*) cross-sectional views of an unit and an array, respectively, and (*c*) top view of an array.

Operation principle

Protein crystals are usually grown from non-equilibrium super-saturated solutions, which contain more proteins than the solvents can dissolve under normal circumstances. As soon as the solubility limits are exceeded, the dissolved proteins do not immediately leave solutions and convert to stable solid-phase particles. Instead, a certain amount of activation energy is required to initiate the formation of solid state. At higher super-saturation, which corresponds to an increased energy state of the system, there is higher probability that critical nuclei will form spontaneously in solution. Under such circumstance, additional tiny nuclei will continue to form, while the growth of existing nuclei remains at a relatively lower rate. On the other hand, stable nuclei may grow in less super-saturated solutions, in which nuclei will rarely spontaneously form. The distributions and ranges of these regions, in which proteins exhibit very different crystallization behaviors, are best illustrated by a simplified phase diagram as shown in figure 1. In a phase diagram, on the vertical axis is the protein concentration of solutions, and along the horizontal axis is the value of a parameter, such as precipitant concentration, pH or temperature, which affects the protein solubility in solutions. For example, as the concentration of precipitant increases, it usually causes a reduction in protein solubility. Although the labile and meta-stable regions are separated by a line in the figure, they are actually regions defined by the probability of spontaneous nucleus formation. In reality, there is no physical discontinuity or distinguishable boundary between these regions. Furthermore, the location and area of these two regions vary noteworthily between different protein solutions. Currently, no general method except trial-and-error is available for locating these regions. In order to grow protein crystals, the first task is therefore to effectively identify the location of the labile and meta-stable regions in the phase space.

When screening for crystallization conditions, protein concentration is gradually raised above the solubility limit to promote the nucleation and growth of protein crystals in the sampled solution. In the most popular hanging drop scheme, separate protein and reference solutions are enclosed in the same chamber. Over the crystallization process, water vapor is driven from protein solution to reference solution because of the concentration difference between them. The final state of the screening is pre-determined and the process is uncontrollable once it proceeds. For our new scheme shown in figure 2, protein solution and reference solution are separated by a semi-permeable membrane, which allows only water but not solutes to pass. Since the direction and flow rate of water across the membrane (and therefore concentrations of the protein solution) can be actively manipulated by adjusting the concentrations (and therefore osmotic pressure) of the reference solution, the new scheme is capable of controlling the crystallization process in a real-time manner. The water flow is controlled by the combination of several factors, including the permeability of the semi-permeable diaphragm, the osmotic pressure and the hydrostatic pressure difference across the semi-permeable diaphragm. The flow rate of water across the semi-permeable diaphragm can be written as the following [15]:

$$J = KA(\sigma \Delta\pi - \Delta P) \tag{1}$$

where J is the flow rate of water (volume of water transported per unit time), K is the permeability of the semi-permeable diaphragm with respect to water, A is the effective surface area of the semi-permeable diaphragm and ΔP is the difference of

the hydrostatic pressure across the semi-permeable diaphragm that has a negative effect on the flow rate. An osmotic reflection coefficient (σ) of the semi-permeable diaphragm is used to account the outward diffusion of the osmotic driving agent through the semi-permeable diaphragm. Ideally, σ equals 1 and no solute will diffuse across. On the other hand, $\Delta\pi$ is the difference of osmotic pressure across the semi-permeable diaphragm that has a positive effect on the flow rate. The osmotic pressure, a chemical potential, of a solution can be represented as follows [15]:

$$\pi = SiRT \tag{2}$$

where S is the concentration of osmotic driving agent, i is the number of ions per mole in the solution, R is the ideal gas constant and T is absolute temperature. Driven by the osmotic pressure difference across the semi-permeable diaphragm, water will flow out or in to raise or lower the concentrations inside the chamber, respectively.

In addition to water and protein molecules, the sampled solutions also contain chemicals such as buffers and precipitants, which are employed to promote and control the crystallization process. For example, the existence of precipitants in the solutions may accelerate the reach of super-saturation, when water is being drained out of the solution. The physical basis of this effect is the competition between protein molecules and precipitant ions in solutions for free water molecules. The precipitant ions increasingly deprive protein molecules of their needed solvent molecules. In other words, precipitants reduce the presence of water without physically removing it from the solution. Therefore, protein molecules initiate association with each another, form clusters and aggregates, and begin to form a solid phase. On the other hand, the solubility limits of protein molecules are usually quite sensitive to pH, which determines the net charge of the protein molecules in solutions. When screen for crystallization conditions, specific types of buffers with a certain range of pH values must be added to maintain fixed charge conditions through the process.

In order to grow diffraction-quality protein crystals, protein solutions are concentrated and brought into super-saturation, in which crystal phase is energetically favorable. In principle, an effective crystallization process must first induce a small number of nuclei after a short period of stay in the labile region, and then switch into the meta-stable region for a long period of incubation to grow the existing tiny nuclei into large crystals. The phase-space trajectories of two osmotic crystallization processes with different initial states are illustrated in figure 1. In our scheme, the continuous draining of water will eventually bring protein solutions into the labile region. Once nucleated, the trajectories then turn down and switch into meta-stable zone for high-quality crystal growth. Throughout the processes, the trajectories can move forward and backward in various speeds when searching the optimal nucleation conditions. In this way, each sample can be screened over extended ranges to achieve a higher hit rate.

Fabrication and screening processes

An assembly diagram of the prototype system, which is composed of polymeric parts, is shown in figure 3.

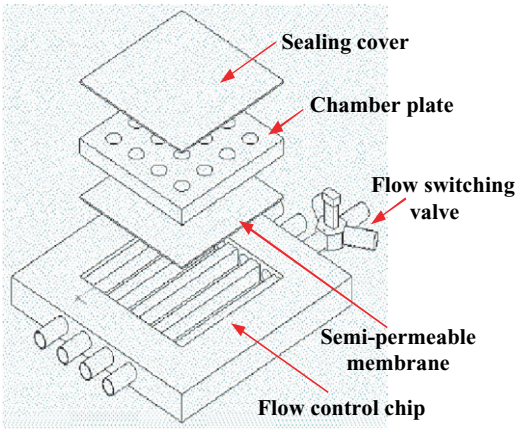

Figure 3. Assembly diagram of the osmotic screening system.

Thermoplastic cellulose acetate is chosen as the membrane material because of its unique semi-permeable property. The semi-permeable membrane is fabricated by solvent casting, in which cellulose acetate is dissolved in acetone and the viscous solution is then dispensed uniformly on a glass plate by a film applicator (Elcometer 3570). The thickness of the deposited semi-permeable membrane, which ranges from tens to hundreds of micrometers, is controlled by the gap between the film applicator and the glass plate. Once acetone is completely evaporated, the transparent cellulose acetate film is peeled off from the plate. In the prototype demonstration, a membrane thickness of 40 μm is employed such that protein crystals can be formed in just hours. On the other hand, the chamber plate is made of a temperature and chemical inert polymer (such as PMMA), and uniformly coated with a thin layer of EVA-based hot melt adhesive (Loctite Hysol 1942) on one surface. By molding or precise milling, through holes with 600 μm in radius and 2 mm in center-to-center spacing are formed on a PMMA plate. The cellulose acetate membrane and the PMMA chamber plate are then rolled (with a constant velocity of 1 mm s^{-1}) and pressed by a hot laminator (at 140 °C) to seal the bottom side of the screening plate. Otherwise, one-piece membrane and cavity assembly can be fabricated by a hot embossing process. Firstly, cylindrical columns with desired dimensions are designed and fabricated on PDMS or silicon substrates. With precise force and displacement control, the hot embossing process can fabricate roughly 1 mm deep chamber with a semi-permeable diaphragm of 150–300 μm in thickness on the backside of the chamber [16]. The prototype systems, 6 × 8 arrays with 6 independent reservoirs underneath, have an overall size of 20 × 24 × 2.5 mm^3 as shown in figure 4.

In this work, sparse-matrix sampling [17], which is arguably the most popular approach for crystallization screening, is employed to search the appropriate crystallization conditions for tested proteins. Originally, this approach uses a set of 50 crystallization solutions, which are chosen based on known or published crystallization conditions for various proteins. In our screening, totally 48 crystallization trails, with 2 initial concentrations of a specific protein, 4 pH values of solutions and 6 precipitating agents including NaCl, $(NH_4)_2SO_4$, $CaCl_2$, Na/K tartrate, Na citrate and PEG 3350 are performed on each array. The details of

Table 1. Crystallization conditions in each of the 48 units on a screening plate.

Conditions→ Precipitants↓	pH = 4.6 C_{p1}	pH = 4.6 C_{p2}	pH = 5.6 C_{p1}	pH = 5.6 C_{p2}	pH = 6.5 C_{p1}	pH = 6.5 C_{p2}	pH = 7.5 C_{p1}	pH = 7.5 C_{p2}
NaCl	#1	#2	#3	#4	#5	#6	#7	#8
$(NH_4)_2SO_4$	#9	#10	#11	#12	#13	#14	#15	#16
$CaCl_2$	#17	#18	#19	#20	#21	#22	#23	#24
Na/K tartrate	#25	#26	#27	#28	#29	#30	#31	#32
Na citrate	#33	#34	#35	#36	#37	#38	#39	#40
PEG 3350	#41	#42	#43	#44	#45	#46	#47	#48

C_{p1} and C_{p2}: two initial protein concentrations with $C_{p1} < C_{p2} <$ solubility limits.

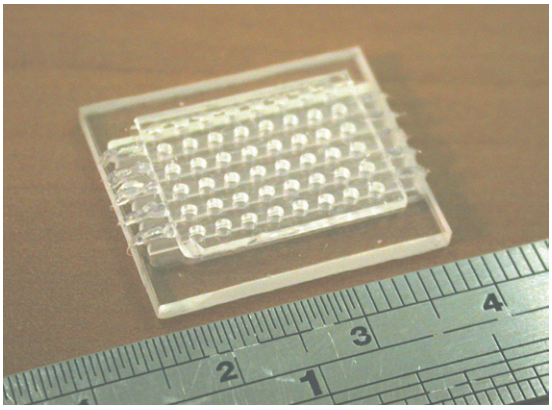

Figure 4. Photograph of the prototype screening system.

the screening experiments are listed in table 1. While screening, the concentrations of protein solutions are controlled by adjusting the precipitant concentrations of underneath reference solutions. These trails are performed at 4 °C (either in a cold room or in a chilling incubator), and inspected under an optical microscope for crystal nucleation and growth. In this work, totally four proteins including lysozyme, catalase, thaumatin and xylanase are used for testing. Before the screening, solutions are prepared and dispensed manually or by a robotic system into the array.

Experimental result

Before performing the screening tests, the flow rates of water across the fabricated 40-μm-thick semi-permeable membrane were first characterized. A glass tube, of 2 mm inside diameter and having one end sealed by the semi-permeable membrane, is filled with more concentrated solution and immersed into another less concentrated solution. The rise of solution level inside the glass tube is measured after 5 h and the flow rate of water across the membrane is calculated by dividing the increment in solution volume by membrane area (3.14 mm^2) and time (5 h). The measured results are listed in table 2, which indicates that water penetration rates, through a membrane with 0.5 M concentration difference across, are higher at higher precipitant concentrations. The measurement errors, which include reading error and the loss of water to outside environment by evaporation and diffusion, are estimated to be less than 3%. Table 3 shows the screening result of lysozyme samples using the proposed osmotic system. The precipitant concentration of reference solutions was initially set at 0.5 M and switched to a higher value once an hour to maintain continuous draining of water out of screening wells. It was observed that after the first hour, protein crystals appeared in well 1, 2, 4, 15 and 32. Afterward, protein crystals were formed in well 3, 6, 13, 22, 23, 24, 25, 26, 27, 31, 39, 41 and 42 after 2 h, and in well 30, 36 and 43 after 3 h. Totally, lysozyme crystals were found in 21 out of the 48 wells in a screening array. Figure 5 shows images of the crystals obtained in the 21 successful trails. The conditions of these successful trails concur with the data revealed by other existing screening techniques. Furthermore, the screening trial was repeated several times to verify its consistency. The results of these trials are almost identical, except that in some cases protein crystals appear earlier or later than expected. These errors are probably caused by the unexpected variations in process temperature, membrane thickness and solution concentrations. In addition to lysozyme, thaumatin samples were also screened by the proposed system to verify its functionality. In this later case, the precipitant concentration of reference solutions was switched once two hours, so the crystallization process proceeds at a lower speed. The result is shown in table 4, which indicates that thaumatin crystals were found in 7 out of the 48 wells in a screening array. Figure 6 shows images of the crystals obtained in the seven successful trails. Furthermore, screening trails with catalase and xylanase also resulted in successful crystal growth as shown in figure 7. In the crystallization experiment, crystals were formed in hours and

Table 2. Measured flow rates of water (nl h^{-1} mm^{-2}) through a 40-μm-thick semi-permeable membrane with fixed concentration differences across the membrane.

Conditions→ Precipitants↓	0.1 M protein solution to 0.5 M reference solution	0.5 M protein solution to 1.0 M reference solution	1.0 M protein solution to 1.5 M reference solution	1.5 M protein solution to 2.0 M reference solution
NaCl	204	230	255	292
$(NH_4)_2SO_4$	228	257	301	345
$CaCl_2$	248	283	327	381
Na/K tartrate	218	252	303	363
Na citrate	221	248	288	331

Table 3. Screening conditions and results for the crystallization of lysozyme.

Precipitant	Conditions → Ref. conc. and time period↓	pH = 4.6 C_{p1}	pH = 4.6 C_{p2}	pH = 5.6 C_{p1}	pH = 5.6 C_{p2}	pH = 6.5 C_{p1}	pH = 6.5 C_{p2}	pH = 7.5 C_{p1}	pH = 7.5 C_{p2}
NaCl	0.5M: 0–1 h	Hit(#1)	Hit(#2)	△	Hit(#4)	△	△	△	△
	1.0M: 1–2 h	○	○	Hit(#3)	○	△	Hit(#6)	△	△
	1.5M: 2–3 h	○	○	○	○	×	○	×	×
	2.0M: 3–4 h	○	○	○	○	×	○	×	×
$(NH_4)SO_2$	0.5M: 0–1 h	×	×	△	△	△	△	Hit(#15)	×
	1.0M: 1–2 h	×	×	△	△	Hit(#13)	×	○	×
	1.5M: 2–3 h	×	×	×	×	△	×	○	×
	2.0M: 3–4 h	×	×	×	×	×	×	○	×
$CaCl_2$	0.5M: 0–1 h	△	△	△	△	△	△	△	△
	1.0M: 1–2 h	△	△	△	△	△	Hit(#22)	Hit(#23)	Hit(#24)
	1.5M: 2–3 h	×	×	×	×	×	○	○	○
	2.0M: 3–4 h	×	×	×	×	×	○	○	○
Na/K tartrate	0.5M: 0–1 h	△	△	△	△	△	△	△	Hit(#32)
	1.0M: 1–2 h	Hit(#25)	Hit(#26)	Hit(#27)	×	△	△	Hit(#31)	○
	1.5M: 2–3 h	○	○	○	×	×	Hit(#30)	○	○
	2.0M: 3–4 h	○	○	○	×	×	○	○	○
Na citrate	0.5M: 0–1 h	△	△	△	△	△	△	△	△
	1.0M: 1–2 h	△	△	△	△	△	△	Hit(#39)	×
	1.5M: 2–3 h	×	×	×	Hit(#36)	×	×	△	×
	2.0M: 3–4 h	×	×	×	○	×	×	×	×
PEG 3350	0.5M: 0–1 h	△	△	△	△	△	△	△	△
	1.0M: 1–2 h	Hit(#41)	Hit(#42)	△	△	△	△	×	×
	1.5M: 2–3 h	○	○	Hit(#43)	×	×	×	×	×
	2.0M: 3–4 h	○	○	○	×	×	×	×	×

$C_{p1} = 32$ mg ml^{-1} and $C_{p2} = 53$ mg ml^{-1}.
△: clear solution, ○: solution with crystals and ×: solution with precipitates.

Table 4. Screening conditions and results for the crystallization of thaumatin.

Precipitant	Conditions → Ref. conc. and time period↓	pH = 4.6 C_{p1}	pH = 4.6 C_{p2}	pH = 5.6 C_{p1}	pH = 5.6 C_{p2}	pH = 6.5 C_{p1}	pH = 6.5 C_{p2}	pH = 7.5 C_{p1}	pH = 7.5 C_{p2}
NaCl	0.5M: 0–2 h	△	△	△	△	△	△	△	△
	1.0M: 2–4 h	△	△	△	△	△	△	△	△
	1.5M: 4–6 h	△	×	△	△	△	△	△	△
	2.0M: 6–8 h	×	×	×	×	×	×	Hit(#7)	×
$(NH_4)SO_2$	0.5M: 0–2 h	△	△	△	△	△	△	△	△
	1.0M: 2–4 h	△	△	△	△	△	×	△	△
	1.5M: 4–6 h	△	△	△	△	×	×	△	△
	2.0M: 6–8 h	×	×	×	×	×	×	×	×
$CaCl_2$	0.5M: 0–2 h	△	△	△	△	△	△	△	△
	1.0M: 2–4 h	△	△	△	×	△	△	△	×
	1.5M: 4–6 h	×	×	×	×	×	×	×	×
	2.0M: 6–8 h	×	×	×	×	×	×	×	×
KNa Tatrate	0.5M: 0–2 h	△	△	△	△	△	Hit(#30)	△	△
	1.0M: 2–4 h	△	△	△	Hit(#28)	Hit(#29)	○	Hit(#31)	Hit(#32)
	1.5M: 4–6 h	×	×	Hit(#27)	○	○	○	○	○
	2.0M: 6–8 h	×	×	○	○	○	○	○	○
Na Citrate	0.5M: 0–2 h	△	△	△	△	△	△	△	△
	1.0M: 2–4 h	△	△	△	△	△	△	△	△
	1.5M: 4–6 h	×	×	×	×	×	×	×	×
	2.0M: 6–8 h	×	×	×	×	×	×	×	×
PEG 3350	0.5M: 0–2 h	×	×	△	△	△	△	△	△
	1.0M: 2–4 h	×	×	△	△	×	×	△	△
	1.5M: 4–6 h	×	×	×	×	×	×	△	△
	2.0M: 6–8 h	×	×	×	×	×	×	×	×

$C_{p1} = 7.5$ mg ml^{-1} and $C_{p2} = 12.5$ mg ml^{-1}.
△: clear solution, ○: solution with crystals and ×: solution with precipitates.

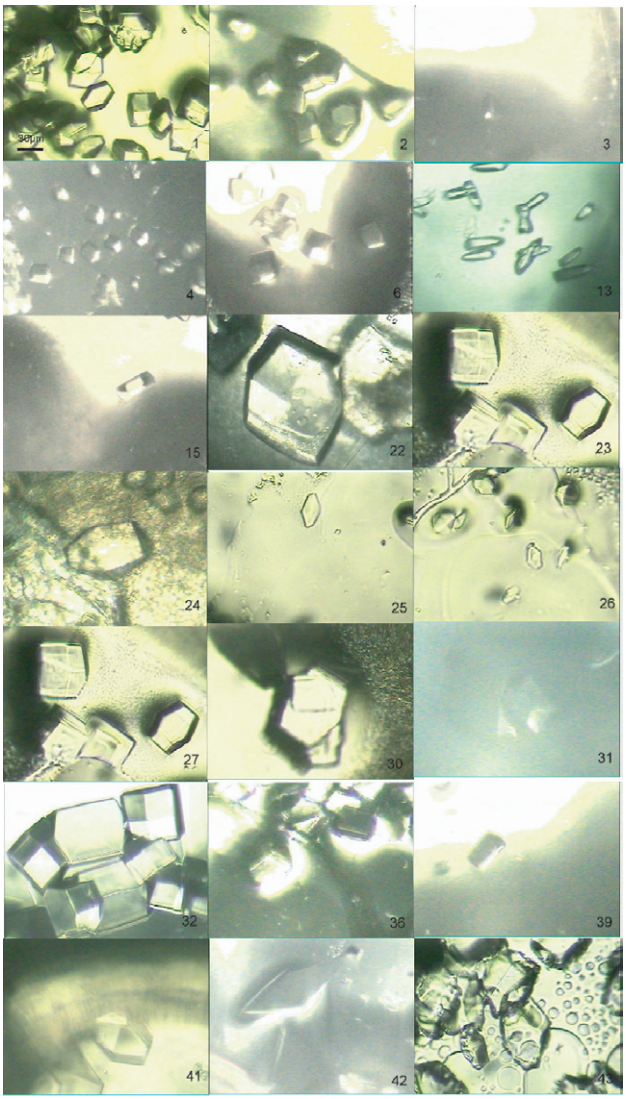

Figure 5. Images of lysozyme crystals in screening chambers after 3 h.

some of them have dimensions larger than 100 μm, which are large enough for x-ray diffraction studies. Large crystals were then extracted, mounted, flash-froze in cryoloops, and subsequently exposed to a laboratory x-ray source. Figure 8 shows a high-resolution diffraction pattern for a single lysozyme crystal grown in our crystallization experiments.

Discussion

In order to grow crystals, protein molecules have to be brought to a super-saturated and thermodynamically unstable state, which may result in a crystalline or amorphous phase once it returns to equilibrium. When raise concentrations to achieve super-saturation and crystallization, the elevating rates have significant impacts on the growth of protein crystals. If concentrations are raised too fast, protein molecules may not respond rapidly enough and may probably miss the opportunity to nucleate at a lower super-saturation, which has a higher

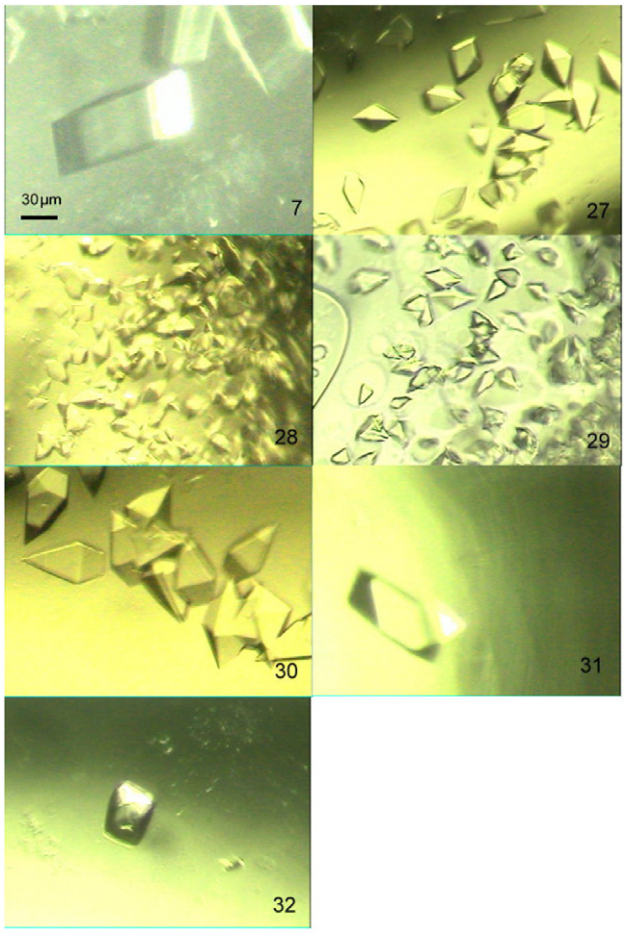

Figure 6. Images of thaumatin crystals in screening chambers after 8 h.

probability of forming diffraction-quality crystals. Instead, a large number of nuclei or even amorphous precipitates may form at a higher super-saturation, which fails to generate usable crystals even though all other conditions are proper for high-quality crystal growth. In the proposed screening system, the raising of protein concentration is achieved by osmosis, which drains water out of protein solutions. According to equation (1), the flow rate of water across the semi-permeable membrane is determined by the osmotic pressure difference across the membrane, the thickness and the effective area of the membrane. Therefore, the elevating profiles of protein concentrations can be pre-programmed by design and fabrication, and fine-tuned by adjusting the concentration difference across the membrane through the crystallization process. In the prototype demonstration, the thickness and effective area of the semi-permeable membrane are about 40 μm and 1 mm^2, respectively, and the flow rate of water out of the protein solution is measured to be in the tens to hundreds of nanoliters per hour range. In case lower elevating rates of protein concentration are needed, either the thickness or the effective area of the semi-permeable membrane can be increased or decreased, respectively, to depress the induced water flow.

Assuming that (1) the difference of the hydrostatic pressure across the semi-permeable diaphragm is much less

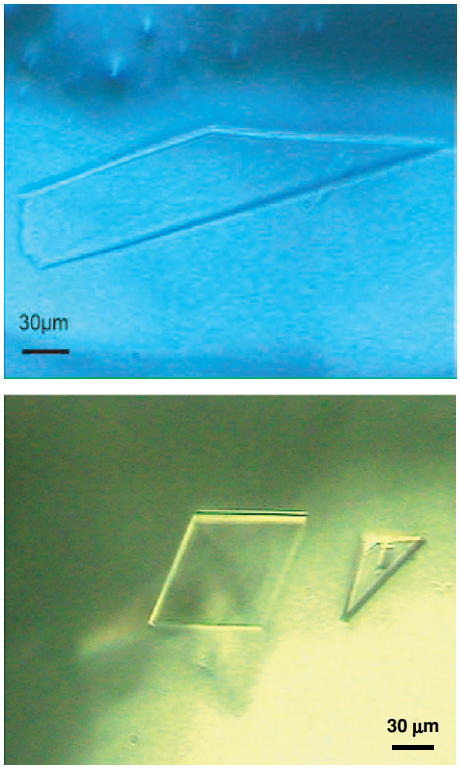

Figure 7. Images of (*a*) catalase and (*b*) xylanase crystals.

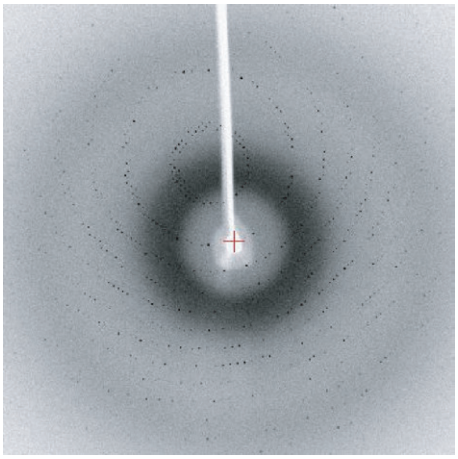

Figure 8. X-ray diffraction pattern from a grown lysozyme crystal.

than that of the osmotic pressure and (2) the precipitant has much higher osmotic pressure than other solutes, when specific membrane material and geometries are employed, the instant flow rate of water across the semi-permeable membrane is approximately proportional to the precipitant concentration difference across the membrane:

$$J(t) = KA\sigma\Delta\pi(t) = K_a(S_i(t) - S_o) \tag{3}$$

where S_i and S_o are the precipitant concentrations of protein and reference solutions, respectively, and K_a is the product of K, A, σ, i, R and T. Because of the large volume of reference solution, S_o can be assumed to be constant throughout the process. Therefore, the instant protein concentration in a screening chamber can be described as:

$$C_i(t) = \frac{C_i(0)V_i(0)}{V_i(0) - \int_0^t K_a\left(\frac{S_i(0)}{C_i(0)}C_i(t) - S_o\right)\mathrm{d}\tau} \tag{4}$$

where C_i and V_i are the protein concentration and the solution volume inside the chamber, respectively. Since the amount of solutes inside the chamber is fixed, the concentrations in the chamber remain raising as water being draining out. The transport of water across a semi-permeable membrane is simulated based on equation (4) and the result is shown in figure 9. Assuming a flow rate of 300 nl h^{-1} (which is approximately the product of the measured flow rate and the area of a membrane of 0.6 mm in radius) at a precipitant concentration difference of 0.4 M (0.1–0.5 M), the protein solution inside the chamber reaches equilibrium with the outside reference solution in roughly 2 h as indicated by the simulation. The rising of concentrations can be divided into two stages. First, the fast decrease of water volume accelerates the rising of concentration, but eventually the decrease in osmotic driving pressure slows down the elevation of concentration and reaches equilibrium at the end. Depending on the characteristics of sampled proteins, the elevation of concentrations can be adjusted by switching the reference concentration accordingly. For proteins such as lysozyme that can be grown under a faster concentration elevation, the switching to higher reference concentrations is performed more frequently to reduce the required crystallization time. In case (such as thaumatin) a slower concentration variation is desired, the reference solution is switched every 2 h or longer with a smaller concentration jump to slow down the outgoing water flow from the screening chambers.

The crystallization process is composed of two stages, the nucleation and growth of protein crystals. In these two stages, the strategies to promote crystallization are different and therefore the conditions should be controlled and optimized accordingly. At the first stage, the concentrations (and super-saturation) are raised slowly and continuously while searching for the lower bound of the labile region. In our scheme, the searching range can be extended deeply into super-saturation (or even precipitation) by repeatedly switching the outside reference solution to a higher precipitant concentration. Currently, the monitoring of crystallization process is done by manual observing under an optical microscope. Once nuclei are detected in the solution, the control of reference solutions is shifted to different schemes. For example, the draining of water is slowed down or even stopped to facilitate a rapid switch from labile to meta-stable region, which prevents nuclei from continuously forming and facilitate the growth from nuclei to larger crystals. In the case that the crystallization is missed at the first trial and amorphous precipitates eventually appear in the protein solution, water can be fed into the solution to dilute and re-dissolve the precipitates for another trial with lower concentration variation. In addition, the screening system can be heated up in an incubator or potentially by an integrated heater with a raised temperature, at which proteins have higher solubility limit, to assist the re-dissolving. As such, protein samples can be tested repeatedly for highly extended crystallization conditions.

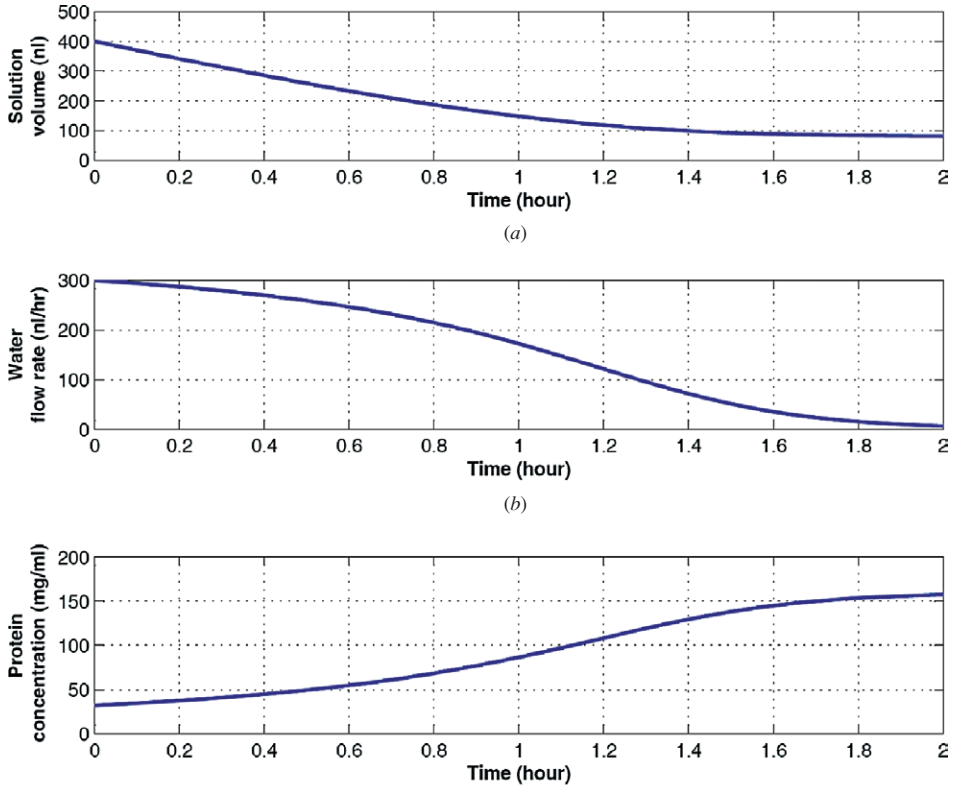

Figure 9. Simulation results of (*a*) solution volume, (*b*) water flow rate and (*c*) protein concentration in the screening cell while water is being drained out by osmosis.

Conclusion

A micro osmotic screening system that grows protein crystals in hours with microgram sample consumption has been successfully demonstrated. The system employs osmosis, which drives water flowing in and out of the sampled protein solution, to adjust concentrations and promote crystallization as desired. As such, each protein sample can be screened for crystallization conditions over highly extended ranges. In the prototype demonstration, 6 × 8 arrays with an overall size of 20 × 24 × 2.5 mm^3 were fabricated and characterized in the crystallization experiments. Crystallization conditions for four proteins, including lysozyme, catalase, thaumatin and xylanase, were identified within 2–6 h while consuming less than 20 μl of sample solution for each protein. X-ray diffraction experiments were also performed and the results indicate that diffraction-quality crystals may be grown and harvested from the proposed osmotic micro-system. As such, this osmotic system pioneers a new class of rapid screening schemes for high-throughput protein crystallization.

Acknowledgments

The authors would like to express their appreciation to Professor Wen-Ching Wang and her search group for their assistance in crystallization and x-ray diffraction experiments. The demonstrated systems were fabricated in the ESS Microfabrication Lab. at National Tsing Hua University, Taiwan. This work is supported in part by the National Science Council of Taiwan under contract no. NSC 94-2218-E-007-050.

References

[1] Burley S K *et al* 1999 Structural genomics: beyond the human genome project *Nature Genetics* **23** 151–7
[2] Blundell T L, Jhoti H and Abell C 2002 High-throughput crystallography for lead discovery in drug design *Nat. Rev. Drug Disc.* **1** 45–54
[3] Babine R E and Abdel-Meguid S S 2004 *Protein Crystallography in Drug Discovery* (Weinheim: Wiley-VCH)
[4] Drenth J 1999 *Principles of Protein X-Ray Crystallography* (New York: Springer)
[5] Abola E, Kuhn P, Earnest T and Stevens R C 2000 Automation of x-ray crystallography *Nat. Struct. Biol.* **7** 973–7
[6] Hosfield D, Palan J, Hilgers M, Scheibe D, McRee D E and Stevens R C 2003 A fully integrated protein crystallization platform for small-molecule drug discovery *J. Struct. Biol.* **142** 207–17
[7] McPherson A 1999 *Crystallization of Biological Macromolecules* (New York: Cold Spring Harbor Laboratory Press)
[8] Ducruix A and Giege R 1999 *Crystallization of Nucleic Acids and Proteins: A Practical Approach* (Oxford: Oxford University Press)
[9] Bergfors T M 1999 *Protein Crystallization: Techniques, Strategies, and Tips* (La Jolla: International University Line)

[10] Stone H A, Stroock A D and Ajdari A 2004 Engineering flows in small devices: microfluidics toward a lab-on-a-chip *Annual Rev. Fluid Mech.* **36** 381–411
[11] Figeys D and Pinto D 2000 Lab-on-a-chip: a revolution in biological and medical sciences *Anal. Chem.* **72** 330A–5A
[12] van der Woerd M, Ferree D and Pusey M 2003 The promise of macromolecular crystallization in microfluidic chips *J. Struct. Biol.* **142** 180–7
[13] Hansen C L, Skordalakes E, Berger J M and Quake S R 2002 A robust and scalable microfluidic metering method that allows protein crystal growth by free interface diffusion *Proc. Natl. Acad. Sci. USA* **99** 16531–6
[14] Zheng B, Roach L S and Ismagilov R F 2003 Screening of protein crystallization conditions on a microfluidic chip using nanoliter-size droplets *J. Am. Chem. Soc.* **125** 11170–1
[15] Theeuwes F and Yum S I 1976 Principles of the design and operation of generic osmotic pumps for the delivery of semisolid or liquid drug formulations *Ann. Biomed. Eng.* **4** 343–53
[16] Su Y C, Lin L and Pisano A P 2002 A water-powered osmotic microactuator *J. Microelectromech. Syst.* **11** 736–42
[17] Jancarik J and Kim S H 1991 Sparse-matrix sampling—a screening method for crystallization of proteins *J. Appl. Cryst.* **24** 409–11